

COMPUTATIONS OF SHIP MANEUVERING IN CALM WATER AND WAVES FOR FULLY APPENDED ONRT MODEL

Jianhua Wang, Decheng Wan*

Computational Marine Hydrodynamics Lab (CMHL), State Key Laboratory of Ocean Engineering,
School of Naval Architecture, Ocean and Civil Engineering, Shanghai Jiao Tong University, Shanghai, China

*Corresponding author: dcwan@sjtu.edu.cn

1. SUMMARY

In the present work, the fully appended ONR Tumblehome ship model is numerically studied for the turning circle maneuver in both calm water and waves. Computations are conducted by CFD code naoe-FOAM-SJTU. Dynamic overset grid technique and 6DoF module with a hierarchy of bodies are used to directly solve the complex motions of the free-running ship maneuvers. The propeller rotational speed is obtained by self-propulsion simulations, where a PI controller is used to update the RPM. CFD results for self-propulsion, maneuvers in calm water and turning circle in waves are presented and compared with the available EFD data. Good agreement with measurement are achieved for both ship motions and the main parameters of self-propulsion and zigzag maneuver, while discrepancies of turning trajectory are observed for the turning circle maneuver. Wave influences on ship maneuverability are also analyzed. Furthermore, flow visualizations including free surface, vortical structures are presented so as to give a better understanding of the hydrodynamic performance of ship maneuvering in calm water and waves.

2. INTRODUCTION

Recently, more and more researchers are paying attention to the hydrodynamic performance of free running ship, especially for the free running ship in waves. Free running ship tests, such as self-propulsion and ship maneuvering tests are very complex regarding to the motions with rotating propellers and turning rudders. When considering ship maneuvering in waves, it will further involve seakeeping performance. Therefore, the evaluation of ship maneuverability for free running ship model is very difficult. For a fully appended ship, it will become more complicated with the modeling and the local flow behaviors around the appendages. So far, free running ship maneuver, especially for ship maneuvering in waves, is one of the most complex problems in the research field of ship hydrodynamics. Previously, different numerical approaches are developed to predict the hydrodynamic performance of ship

maneuverability and ship maneuvering in waves, but it still challenging to give accurate predictions.

Among several numerical models, mathematical models are widely used to predict the maneuvering motion. And for the wave effects, potential theory are applied to calculate the wave induced motions. Zhang and Zou[1,2] used the 4 degrees of freedom (4DoF) mathematical model MMG to solve ship maneuvering motion and the high frequency wave induced motions were solved by a linearized time domain potential flow method. The numerical results showed a large discrepancy with experimental data, which showed that the MMG model associated with potential theory cannot accurately describe the maneuvering characters in waves. Seo and Kim[3] adopted a similar approach to model the maneuvering motion in waves. The predicted results showed reasonable agreement but still less accuracy. It can be noticed that the superposition approach based on mathematical model and potential theory cannot give accurate prediction due to the simplification of the coupling effects between waves and free running ship. Therefore, computational fluid dynamics (CFD) method is more reliable in the direct predictions of ship maneuvering and seakeeping performances. CFD simulations can provide accurate and sufficient prediction of hydrodynamic forces and local flow details around the ship hull and its complex appendages. However, considering the high computational cost and complex numerical models, only a small number of free-running simulations have been done by direct CFD method, and the number is even less for the free-running ship maneuvers in waves.

Up to now, the most reliable and widely used approach to simulate free-running ship maneuver is the dynamic overset grid method. Carrica et al.[4] simulated the turn and zigzag maneuver by using a Reynolds-Average Navier-Stokes (RANS) approach where the deflection of rudders were achieved by the dynamic overset grid technique, while the rotating propellers were simplified by body forces. In addition, the authors also performed simulations of ship maneuvering in waves based on the simplified body force

model and found that the main discrepancy between the CFD and EFD can possibly due to the simplistic propeller model. Broglia et al.[5] and Dubbioso et al.[6] adopted a similar overset grid approach to simulate the turning circle maneuver in calm water. The ship model was a fully appended twin-screw vessel with a single rudder and the twin rotating propellers were simulated by an actuator disk model. Further analysis for the hydrodynamic loads acting on the hull and appendages was presented for the turning circle maneuver simulations. Shen et al.[7] implemented the dynamic overset grid module to OpenFOAM and presented numerical applications to the self-propulsion and zigzag maneuver simulations of KCS model. Their results agreed well with the experimental data, which proved that the fully discretized model with overset grid method was reliable.

Except the studies on ship maneuver with free-running ship models in calm water, there are several applications for the CFD simulations of ship maneuvering in waves. Wang et al. [8,9] conducted the free-running simulations for course-keeping maneuver and zigzag maneuver in various wave conditions. Liu et al.[10] used the dynamic overset grid method to predict turning circle maneuver in waves for DTC ship. Their results showed that the CFD computations for ship maneuvering in waves was feasible and reliable. In the present paper, computations of benchmark cases in SIMMAN 2020 are conducted focusing on ONRT ship self-propulsion, turning circle maneuver in both calm water and waves.

This paper is organized as follows: the numerical methods are presented in the second section; the computational overviews, including the geometry model, test conditions and numerical grids are described in the third section; the numerical results and discussions are presented in the fourth section; finally, brief conclusions from the present study are drawn.

3. NUMERICAL METHODS

3.1 CFD Solver

The present computations are based on the in-house CFD solver naoe-FOAM-SJTU [11]. The solver is developed for complex marine hydrodynamic problems. The main feature of naoe-FOAM-SJTU solver is the self-developed modules in OpenFOAM, including dynamic overset grid and 6DoF motion module with a hierarchy of bodies [7], which is very convenient to conduct direct CFD simulations of free running ship maneuvers. Other modules of the solver include a 3D numerical wave tank [12,13] for wave generation and absorption, a mooring system module [14], delayed detached eddy simulation module [15], etc. So far, the CFD solver has been successfully applied to predict the hydrodynamic performance of ship resistance and wave-making [16], seakeeping [17,18], propulsion [19], maneuverability [11] and ship maneuvering in waves [8,9,20].

3.2 Numerical Schemes

Reynold-Averaged Navier-Stokes equations for unsteady, incompressible, immiscible two-phase flows are solved in the simulations for ship maneuvers. An algebraic volume of fluid (VOF) method coupled with artificial compression technique [21] in OpenFOAM is used to capture the free surface. Numerical wave tank based on relaxation technique is applied to generate wave environment. Turbulence is modelled with the standard shear stress (SST) $k-\omega$ two-equation model [22]. Built-in discretization schemes in OpenFOAM are employed to solve the partial differential equations. PISO algorithm [23] is applied for pressure-velocity coupling in solving governing equations.

4. COMPUTATIONAL OVERVIEWS

4.1 Geometry Model

The fully appended ONR Tumblehome (ONRT) ship model is used for all the self-propulsion and turning circle simulations. The ship model is fitted with skeg bilge keels, shaft, brackets and rudder root. The geometry model of ONRT is shown in Figure 1, and the main particulars are listed in Table 1. This ship model is 3.048m long and it is used as one of the benchmark ship models in SIMMAN 2020 workshop. The available experimental results provided by SIMMAN can be used to validate our CFD simulations.

Table 1 Main particulars of ONRT ship model

| Main particulars | | Model scale | Full scale |
|-----------------------|----------------------|-------------|------------|
| Length of waterline | $L_{wl} (m)$ | 3.147 | 154.0 |
| Beam of waterline | $B_{wl} (m)$ | 0.384 | 18.78 |
| Draft | $T (m)$ | 0.112 | 5.494 |
| Displacement | $\Delta (kg)$ | 72.6 | 8.507e6 |
| Block coefficient | | 0.535 | 0.535 |
| Propeller diameter | $D_p (m)$ | 0.1066 | NA |
| Propeller shaft angle | $\varepsilon (deg.)$ | 5 | NA |
| Propeller rotation | | inward | inward |
| Max rudder rate | deg./s | 35 | 5 |



Figure 1 Geometry of ONRT ship model

4.2 Computational Grids

Dynamic overset grids are used to discretize the fully appended twin-screw ONRT ship. In order to directly handle the large amplitude ship motions and twin rotating

propellers and turning rudders, the computational domain for all the cases is divided into six overlapping regions: background, ship hull, two for propellers and another two for twin rudders. For self-propulsion and maneuvers in calm water case, a rectangular domain is adopted, while a circular domain is adopted for turning circle in waves. The different computational domain is shown in Figure 2.

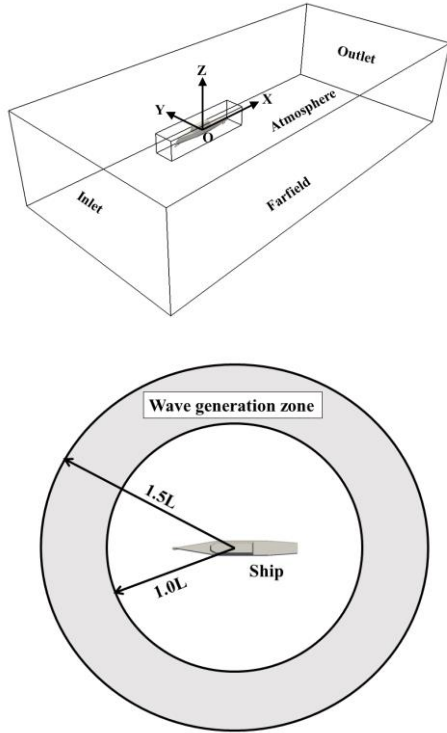


Figure 2 Computational domain (upper: self-propulsion and turning circle in calm water; lower: turning circle in waves)

All grids used in this paper are generated by HEXPRESS and the total grid number of the simulation is 7.34M and 7.13M for calm water and wave case, respectively. It should be noted that artificial gaps between propeller and shaft, rudder and rudder root are used to obtain enough interpolation cells. Local grid distribution around ship hull, propeller and rudder is shown in Figure 3. The y^+ value is around 30-40 along the hull surface with the consideration of wall functions are applied in the near wall region.

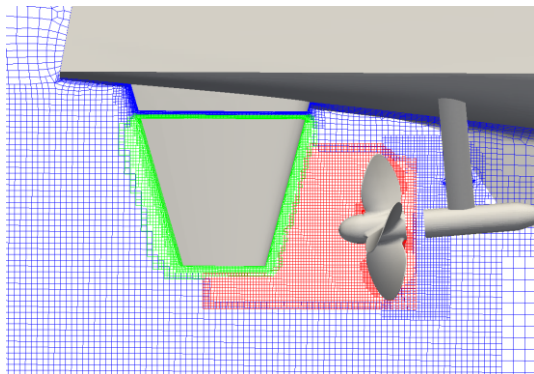


Figure 3 Local grid distribution

4.3 Test Conditions

According to the benchmark cases in SIMMAN 2020 workshop, the present simulations are based on case 5.2 and case 5.3. The self-propulsion simulation is firstly conducted to get the model point, and then the RPM is fixed for the simulations of maneuvers in calm water and turning circle in waves. Ship speed is 1.11m/s, corresponding to $Fr=0.20$. During the simulations, all the 6 degrees of freedom are considered.

5. RESULTS AND DISCUSSIONS

Numerical computations are carried out on the HPC cluster center in Computational Marine Hydrodynamics Lab (CMHL), Shanghai Jiao Tong University. Each node consists of 2 CPUs with 20 cores per node and 64GB accessible memory (Intel Xeon E5-2680v2 @2.8 GHz). 40 processors are assigned to calculate the self-propulsion and maneuver in calm water case, in which 39 processors are assigned for the flow calculation and the other one processor is applied for the DCI computation using overset grids. 60 processors are used for the wave case.

5.1 Self-propulsion

Self-propulsion case is used to validate our CFD solver and also used to obtain the self-propulsion model point. The present simulation follows the benchmark case 5.2.1 in SIMMAN 2020 workshop. During the simulation, the rate of revolutions of the propeller n is to be adjusted to obtain the force equilibrium in the longitudinal direction by a PI controller [7]. The proportional and integral value is set to $P=800$ and $I=800$, respectively, with the consideration of larger constants can accelerate the computations and the convergence of the propeller revolution rate. The computation starts from the steady state of towing condition and the ship model is then released in 6 degrees of freedom following the experiment setup.

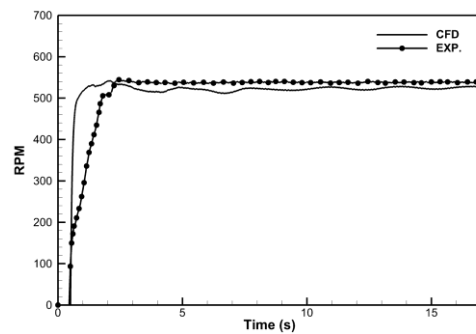


Figure 4 Time histories of RPM and its comparison with experimental data

Figure 4 presents the comparison between time histories of computed rotational speed of propeller (Rate per Minute, RPM) and experimental measurement. The predicted RPM is 525 and is under-estimated by 2.4% compared with experimental result of 538. The numerical results are very

promising and it indicates that the present numerical approach is reliable in predicting free running ship. The present predicted model point is then applied in the following computations of maneuvers in calm water and turning circle maneuver in waves.

5.2 20/20 Zigzag Maneuver

Benchmark case for maneuvers in calm water includes two different cases, one is the standard 20/20 zigzag maneuver and another one is the 35 degree turning circle maneuver. This section illustrates the numerical results of zigzag maneuver. As mentioned in self-propulsion simulation, the RPM is fixed during the maneuver simulations. According to the case description, the maneuver starts with starboard side rudder. Figure 5 shows the computed results of the time histories of heading angle and rudder deflection. It can be clearly seen that the predict results show an overall agreement with the experiments, where the overshoot angles are underestimated. Another phenomenon can be observed is that there is a phase lag for the predicted results.

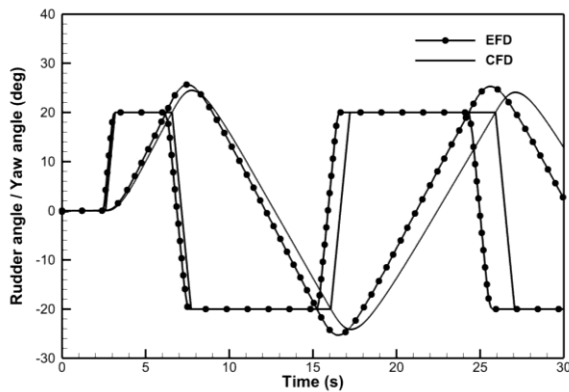


Figure 5 Comparison of time histories of rudder deflection and yaw angle in 20/20 zigzag maneuver

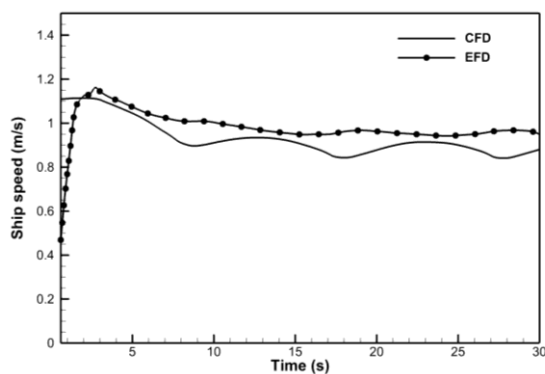


Figure 6 Comparison of instantaneous ship speed

In order to find out how the phase lag comes, we have plotted the time histories of instantaneous ship speed during zigzag maneuver in calm water shown in Figure 6. It is very obvious that the predicted ship speed is underestimated and this is mainly due to the RPM applied in the present computations are not exactly the same with the experiment. It is also very hard to reappear the actual states of the test in

the simulations. However, the present method can give a relatively good prediction of the standard zigzag maneuver.

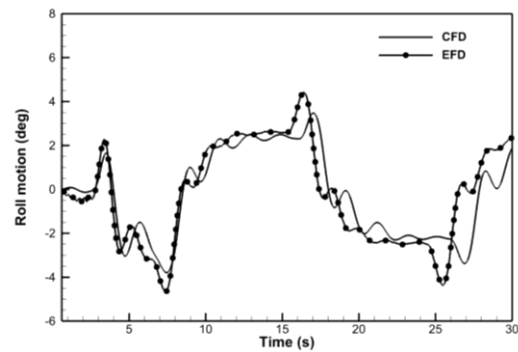


Figure 7 Comparison of roll motion

Figure 7 demonstrates the comparison of roll motion during the 20/20 zigzag maneuver. The CFD data is very promising when compared with the measurement, while the discrepancy for the phase lag can also be observed. The peak value for the roll motion is underestimated, but the overall fluctuation characters can be captured.

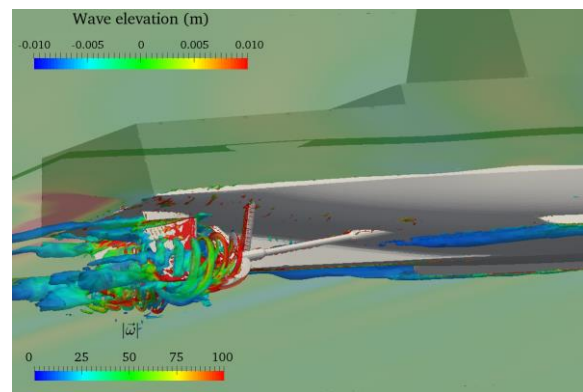


Figure 8 Snapshots of the vortical structures around ship propellers and rudders

Despite the predicted data, the present CFD computations can also give detailed and abundant flow information to describe the complex flows during ship maneuvering motion. Figure 8 depicts the vortical structures around twin rotating propellers and turning rudders during 20/20 zigzag motion. The iso-surfaces are using the new vortex identification approach [24] to give a better description of both strong and weak vortices. The weak vortices separated from bilge keels, strong tip vortices from propeller blade and rudder vortices can be well resolved. Strong interactions between propeller vortices and the aligned rudder are occurred. These abundant flow data can be used to give an insight view of the hydrodynamic performance during the maneuvering motion.

5.3 Turning Circle Maneuver in Waves

The benchmark case 5.3 for ship maneuver in waves is the standard 35 degree turning circle maneuver starting to portside. In the present simulations, the computations starts from steady state of self-propulsion case, and then the

waves are generated from the circular relaxation zone. The option for the circular domain is mainly due to the turning circle maneuver will experience 360 degree turning, thus the circular relaxation region can avoid the wave passing out the domain. However, due to the high computational cost for maneuvering in waves, here we only use a relatively small domain. The simulations are performed for the turning maneuver starting to starboard side and all the simulation results will be mirrored to give quantitative comparisons corresponding to the experiments.

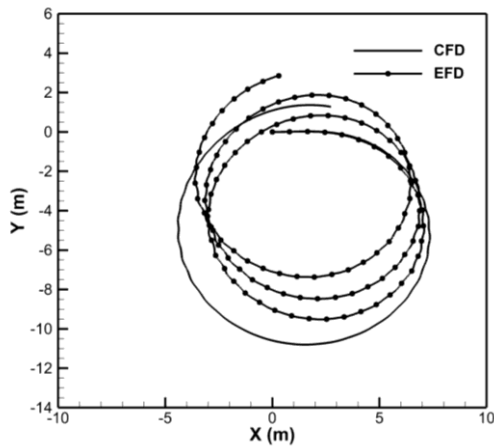


Figure 9 Comparisons of turning trajectory

Figure 9 illustrates the comparison of turning trajectory during 35 degree turning circle maneuver in waves. The present numerical simulations only performed for one circle and it can be observed that our CFD results show relatively large discrepancies for the turning diameter, while the local fluctuations due to the wave effects can be captures around beam sea states. The predicted turning diameter is about 11.8m, which is overestimated by 15.9% comparing with the experimental data of 10.18m. This large discrepancy can be caused by several reasons. One reason is the small computational domain, which can barely capture the drift behavior and the wave reflection cannot be avoided in the simulations. Another reason responsible for the discrepancy can be the RANS approach, which may not suitable for the large rudder deflection case and the vortices separated from the hull and rudder are much more complicated.

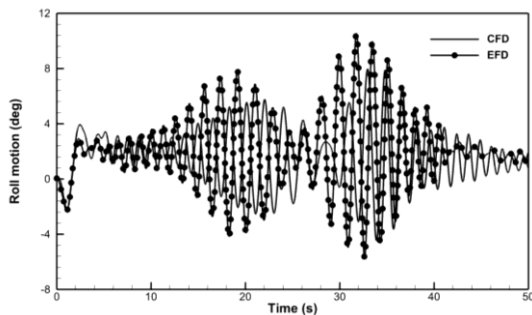


Figure 10 Comparison of roll motion during turning circle maneuver in waves

Figure 10 and Figure 11 illustrate the time histories of roll motion and pitch motion during the turning circle in waves. It can be clearly observed that even though the trajectory has a large discrepancy, the present computations can still give an overall agreement with the time variations of wave-induced motions. The high frequency fluctuations are due to the incident waves and the low frequency fluctuations are caused by the turning motion. Since the turning trajectory has a different behavior between CFD and EFD, the low frequency fluctuations has a corresponding delay in phase.

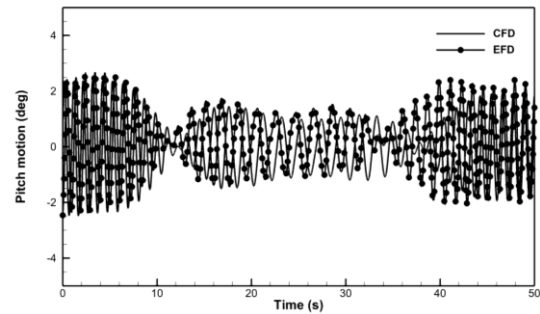


Figure 11 Comparison of pitch motion during turning circle maneuver in waves

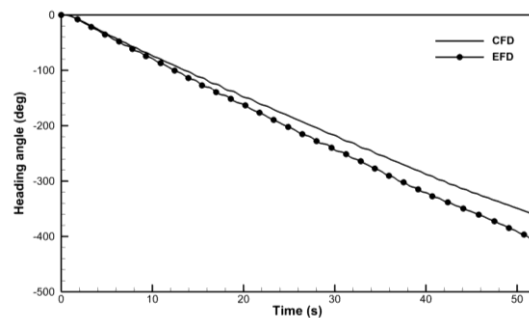


Figure 12 Comparisons of heading angle

Figure 12 also shows the comparisons of heading angle of the ship model during turning circle motion in waves. It can be noticed that the time to complete one circle is 51.8s and 45.7s in model scale for CFD and EFD, respectively. The period for the turning circle in waves is overpredicted by 13.3%. It means that the turning ability is less in the CFD model and this is also consistent with the predictions in zigzag maneuvers.

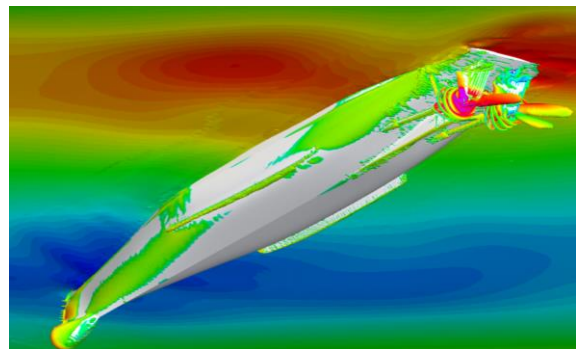


Figure 13 Vortical structures for turning circle maneuver in waves

Figure 13 gives a global view of the flow field during turning circle maneuver in waves, representing by the iso-surface of vorticity. The strong interactions between propeller and rudder, as well as the wave-hull interaction can be clearly observed.

6. CONCLUSIONS

The present paper shows the numerical results for ship self-propulsion, maneuvers in both calm water and waves. Twin-screw fully appended ship model is simulated using naoe-FOAM-SJTU solver. Self-propulsion model point can be accurately predicted with an error lower than 3%. The main parameters for zigzag maneuver in calm water can also be well predicted and the time histories of ship motions and yaw rates show good agreement with the measurements. Large discrepancies for turning circle maneuver in waves is observed, with the error up to 15.9% for the turning diameter. The small computational domain and the RANS model is possibly responsible for the deviation. Future work will be done to find a more accurate prediction approach for the turning circle maneuver in waves.

ACKNOWLEDGEMENTS

This work is supported by the National Natural Science Foundation of China (51879159), The National Key Research and Development Program of China (2019YFB1704200, 2019YFC0312400), Chang Jiang Scholars Program (T2014099), Shanghai Excellent Academic Leaders Program (17XD1402300), and Innovative Special Project of Numerical Tank of Ministry of Industry and Information Technology of China (2016-23/09), to which the authors are most grateful.

REFERENCES

- [1] Zhang, W., and Zou, Z. "A Numerical Study on Prediction of Ship Maneuvering in Waves," Proc. of 30th IWWWFB, Bristol, UK, 2015
- [2] Zhang, W., and Zou, Z. "Time Domain Simulations of the Wave-Induced Motions of Ships in Maneuvering Condition," J. Mar. Sci. Technol., **21**(1), pp. 154–166, 2016
- [3] Seo, M.-G., and Kim, Y. "Numerical Analysis on Ship Maneuvering Coupled with Ship Motion in Waves," Ocean Eng., **38**(17), pp. 1934–1945, 2011
- [4] Carrica, P. M., Ismail, F., Hyman, M., Bhushan, S., and Stern, F. "Turn and Zigzag Maneuvers of a Surface Combatant Using a URANS Approach with Dynamic Overset Grids," J. Mar. Sci. Technol., **18**(2), pp. 166–181, 2012
- [5] Broglia, R., Dubbioso, G., Durante, D., and Di Mascio, A. "Turning Ability Analysis of a Fully Appended Twin Screw Vessel by CFD. Part I: Single Rudder Configuration," Ocean Eng., **105**, pp. 275–286, 2015
- [6] Dubbioso, G., Durante, D., Di Mascio, A., and Broglia, R. "Turning Ability Analysis of a Fully Appended Twin Screw Vessel by CFD. Part II: Single vs. Twin Rudder Configuration," Ocean Eng., **117**, pp. 259–271, 2016
- [7] Shen, Z., Wan, D.C., and Carrica, P. M. "Dynamic Overset Grids in OpenFOAM with Application to KCS Self-Propulsion and Maneuvering," Ocean Eng., **108**, pp. 287–306, 2015
- [8] Wang, J., Zou, L., and Wan, D.C. "CFD Simulations of Free Running Ship under Course Keeping Control," Ocean Eng., **141**, pp. 450–464, 2017
- [9] Wang, J., Zou, L., and Wan, D.C. "Numerical Simulations of Zigzag Maneuver of Free Running Ship in Waves by RANS-Overset Grid Method," Ocean Eng., **162**, pp. 55–79, 2018
- [10] Liu, C., Wang, J., and Wan, D.C. "CFD Simulations of Self-Propulsion and Turning Circle Manoeuvre in Waves," Proc. of 32nd SNH, Hamburg, Germany, 2018
- [11] Wang, J., Zhao, W., and Wan, D.C. "Development of Naoe-FOAM-SJTU Solver Based on OpenFOAM for Marine Hydrodynamics," J. Hydrodyn., **31**(1), pp. 1–20, 2019
- [12] Cao, H., and Wan, D.C. "Development of Multidirectional Nonlinear Numerical Wave Tank by Naoe-FOAM-SJTU Solver," Int. J. Ocean Syst. Eng., **4**(1), pp. 52–59, 2014
- [13] Shen, Z., and Wan, D.C. "An Irregular Wave Generating Approach Based on Naoe-FOAM-SJTU Solver," China Ocean Eng., **30**, pp. 177–192, 2016
- [14] Liu, Y., and Wan, D.C. "Numerical Simulation of Motion Response of an Offshore Observation Platform in Waves," J. Mar. Sci. Appl., **12**(1), pp. 89–97, 2013
- [15] Zhao, W., Zou, L., Wan, D.C., and Hu, Z. "Numerical Investigation of Vortex-Induced Motions of a Paired-Column Semi-Submersible in Currents," Ocean Eng., **164**, pp. 272–283, 2018
- [16] Wang, J., Ren, Z., and Wan, D.C. "Study of a Container Ship with Breaking Waves at High Froude Number Using URANS and DDES Methods," J. Ship Res, 2020
- [17] Liu, C., Wang, J., and Wan, D.C. "CFD Computation of Wave Forces and Motions of DTC Ship in Oblique Waves," Int. J. Offshore Polar Eng., **28**(02), pp. 154–163, 2018
- [18] Shen, Z., and Wan, D.C. "RANS Computations of Added Resistance and Motions of a Ship in Head Waves," Int. J. Offshore Polar Eng., **23**(04), pp. 264–271, 2013
- [19] Wang, J., Zhao, W., and Wan, D.C. "Simulations of Self-Propelled Fully Appended Ship Model at Different Speeds," Int. J. Comput. Methods, **16**(3), pp. 1840015-1–22, 2019
- [20] Wang, J., and Wan, D.C. "CFD Investigations of Ship Maneuvering in Waves Using Naoe-FOAM-SJTU Solver," J. Mar. Sci. Appl., **17**(3), pp. 443–458, 2018
- [21] Berberović, E., van Hinsberg, N., Jakirlić, S., Roisman, I., and Tropea, C. "Drop Impact onto a Liquid Layer of Finite Thickness: Dynamics of the Cavity Evolution," Phys. Rev. E, **79**(3), p. 36306, 2009
- [22] Menter, F. R., Kuntz, M., and Langtry, R. "Ten

Years of Industrial Experience with the SST Turbulence Model,” *Turbul. Heat Mass Transf.*, **4**(1), pp. 625–632, 2003

[23] Issa, R. I. “Solution of the Implicitly Discretised Fluid Flow Equations by Operator-Splitting,” *J. Comput. Phys.*, **62**(1), pp. 40–65, 1986

[24] Liu, J., and Liu, C. “Modified Normalized Rortex/Vortex Identification Method,” *Phys. Fluids*, **31**(6), p. 061704, 2019